01 Jan 1972

A Strain Energy Comparison Of Discrete Modeling For Vibrating Continuous Systems

S. K. Tolani

Richard Dale Rocke
Missouri University of Science and Technology

Recommended Citation

S. K. Tolani and R. D. Rocke, "A Strain Energy Comparison Of Discrete Modeling For Vibrating Continuous Systems," *Journal of Manufacturing Science and Engineering, Transactions of the ASME*, vol. 94, no. 1, pp. 23 - 30, American Society of Mechanical Engineers, Jan 1972.
The definitive version is available at https://doi.org/10.1115/1.3428117

S. K. TOLANI
Graduate Student.

R. D. ROCKE
Associate Professor.
Mem. ASME

Department of Mechanical and Aerospace Engineering, University of Missouri—Rolla, Rolla, Mo.

A Strain Energy Comparison of Discrete Modeling for Vibrating Continuous Systems

Lumped parameter models commonly used to describe continuous one-dimensional and Bernoulli-Euler beam vibration problems have been compared on the basis of maximum system strain energy. The consistent mass matrix approach has been included in the comparison. Standard matrix techniques have been employed to mathematically obtain desired solutions. Closed form solutions and solutions via the models to the system strain energy were obtained for all systems in three dynamic states: Free vibrations, constant base acceleration, and half sine base acceleration. Behavior of the strain energy errors, in general, were found to be similar to those of the frequency root errors.

Introduction

Most vibration problems involve continuous elements, but few are treated, in practice, on the basis of continuum theory. The most common approach is to model the elements of a structure, i.e., replace the continuum by a multi-degree of freedom discrete structure, and then solve the set of governing total differential equations exactly. The solutions obtained in this manner, however, will not be exact because of error created in the modeling and errors made during numerical manipulations of the equations. Examination of the modeling error is of primary concern herein.

The terminology applied to the process of replacing continuous elements by discrete ones, such as massless springs and point masses, has for some years been called lumped parameter modeling. The more recent work of this type during the past few years has been termed the finite element approach. The work reported herein includes both lumped parameter and finite element models as applied to continuous systems governed by the one-dimensional wave equation and the Bernoulli-Euler beam equation.

The lumped parameter technique was first applied by Lagrange [1][1] and Rayleigh [2] in studying the vibrating string. Duncan [3], using a lumped parameter model attributed to Lagrange, was one of the first to study the behavior of errors resulting from the use of lumped parameter approximations. Rocke [4–5] evaluated one-dimensional models using a transmission matrix approach and showed improvement to the basic Duncan model.

Several investigators [6–9] have evaluated lumped parameter approximations of uniform continuous beams using many different models. Use of the consistent mass matrix within the finite element approach has been evaluated by Archer [10] and several other investigators [11–12].

A suitable model is one for which successively finer subdivisions of a system leads to a convergence to the exact solution, the best model being the one which provides the required accuracy for a minimum of computational effort. The basis of accuracy comparison for dynamic systems has to date been that of the principal

Contributed by the Design Engineering Division and presented at the Vibrations Conference, Toronto, Canada, September 8–10, 1971, of The American Society of Mechanical Engineers. Manuscript received at ASME Headquarters, May 11, 1971. Paper No. 71-Vibr-5.

[1] Numbers in brackets designate Reference at end of paper.

Nomenclature

A = area of cross section of the system
EI = bending stiffness of the beam
$f_r(t)$ = time dependent part of the displacement function in the rth mode
$[\backslash J \backslash]$ = diagonal inertia matrix of the beam
k = spring stiffness
$[K]$ = stiffness matrix
l = length of each segment
L = length of the system
m = mass of each segment
$[M]$ = mass matrix
$[\backslash M \backslash]$ = diagonal mass matrix
$\{M_i\}$ = lumped masses as a column vector
N = number of segments
t = time
$u(x, t)$ = displacement function for one-dimensional systems
U_i = maximum system strain energy in the ith mode
$U(t)$ = system strain energy
$\{x\}$ = coordinate displacement vector
$\{\bar{x}\}$ = relative coordinate vector
$y_r(x, t)$ = displacement function for beams
$\{\theta\}$ = beam rotation vector
$[\nu]$ = normalized modal matrix of the system
ρ = mass per unit length of the system
$\phi_n(x)$ = nth mode shape function
ω_i = circular frequency in the ith mode

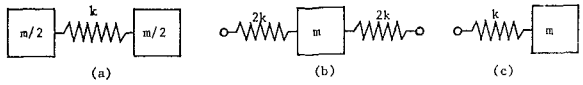

Fig. 1 Lumped parameter models for uniform one-dimensional systems

mode frequency root errors. However, these comparisons do not insure that the free or forced vibration solution, in total, is more accurately produced by the model judged best on the basis of principal mode frequency root errors.

The objective of the work herein was to provide a consistent basis of comparison for models representing systems in a general dynamic state. The basis used was that of the maximum system strain energy. Strain energy being proportional to the stress times strain summed over the entire system should be indicative of system displacements and stresses independent of their position within the system. Furthermore, the maximum system strain energy should be a better measure of total system distortion than any one particular parameter, i.e., maximum displacement or maximum stress.

Lumped Parameter Models

A One-Dimensional Systems. Systems represented by the one-dimensional wave equation, i.e., longitudinal vibrations of bars, torsional oscillations of shafts, transverse vibrations of strings, acoustical oscillations in ducts, etc., have the same solution within the constants or parameters which are basic to that system's description. For simplicity the longitudinal rod with appropriate constants is used as illustrative of this group.

Three types of lumped parameter models, as shown in Fig. 1, have been used to describe the longitudinal rod. These models each approximate the mass and stiffness of one increment of a uniform continuous rod composed of N equal segments. Model (*a*) was first used by Rayleigh and model (*b*) has been attributed in the literature to Lagrange but has been investigated to some extent by Duncan. Model (*c*) has been used to a large extent in practice. Appendix A shows the general forms of mass and stiffness matrices for models (*a*), (*b*), and (*c*) for a *N*-segmented rod. Fixed-fixed and fixed-free boundary conditions were investigated as these two types have shown the largest discrepancy in frequency root error behavior among the three models.

B Bernoulli-Euler Beam Models. Evaluation of lumped parameter models for the uniform Bernoulli-Euler beam has received much more attention in the literature than those for the one-dimensional systems. Two of the models judged best on the basis of principal mode frequency root errors are shown in Fig. 2. Livesly [6] and Gladwell [7] have examined these two models to describe their frequency root error behavior as a function of N for different boundary conditions. The fixed-fixed and fixed-free cases are included in this comparison because they have shown the greatest differences in frequency root error behavior.

Appendix B gives the general stiffness matrix forms for the two beam models when used to describe a uniform beam divided into N equal segments. The mass matrices are diagonal and similar to those for the one-dimensional models. It should be noted that models (*a*) and (*b*) both include only mass and no rotary inertia; hence, they describe directly only transverse displacements of the beam element. The technique used to obtain the matrix equations in terms of transverse displacements only is illustrated in Appendix D.

C Consistent Mass Matrix Approach. This technique [11–12] has been used for both the one-dimensional and Bernoulli-Euler beam elements and differs from the lumped parameter models being used only in that the inertia forces are considered to be distributed in the element rather than concentrated at the discrete coordinate points. Distributing the inertia forces causes the mass matrix to be nondiagonal as shown in Appendix C. The

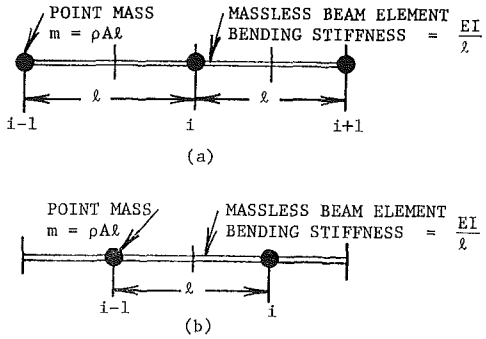

Fig. 2 Lumped parameter models for uniform beams

consistent mass matrix approach was used to describe the same cases as used with the lumped parameter models for direct comparison.

Governing Equations for Lumped Parameter Models

A Homogeneous Equations. The differential equations of motion in matrix form for the homogeneous solutions via all of the lumped parameter models are given by:

$$[\diagdown M \diagdown]\{\ddot{x}\} + [K]\{x\} = \{0\}, \tag{1}$$

where $\{x\}$ are the absolute displacements of the coordinate points in a Newtonian reference frame, i.e., in the lumped parameter cases the mass displacements. Using $\{x\} = [\diagdown M \diagdown]^{-1/2}\{\delta\}$, i.e., a change of system coordinates, and substitution into equation (1) with a premultiplication by $[\diagdown M \diagdown]^{-1/2}$ gives:

$$\{\ddot{\delta}\} + [\bar{K}]\{\delta\} = \{0\}, \tag{2}$$

where:

$$[\bar{K}] = [\diagdown M \diagdown]^{-1/2}[K][\diagdown M \diagdown]^{-1/2}.$$

Eigenvalues of $[\bar{K}]$ are the same as those of $[K]$ but the modal matrix for equation (1) becomes:

$$[\mu] = [\diagdown M \diagdown]^{-1/2}[\beta],$$

where $[\beta]$ is the modal matrix of equation (2). A normalized modal matrix $[\nu]$ of equation (1) was obtained through a normalization such that the product $[\nu]^T[\diagdown M \diagdown][\nu]$ is equal to the total mass of the system, i.e.,

$$[\nu] = [\mu][\diagdown A_i \diagdown]; \quad [\diagdown A_i \diagdown] = (Nm)^{1/2}[[\mu]^T[\diagdown M \diagdown][\mu]]^{-1/2} \tag{3}$$

and these normalized modes were used to obtain principal mode strain energies.

B Forced Excitation Solutions. For systems with base acceleration excitation the equations of motion in matrix notation are given by:

$$[\diagdown M \diagdown]\{\ddot{\bar{x}}\} + [K]\{\bar{x}\} = -\ddot{u}_B(t)\{M_i\} \tag{4}$$

where $\{\bar{x}\}$ are coordinates relative to the base and $\ddot{u}_B(t)$ is a general time-varying base acceleration, i.e.,

$$x_i = u_B(t) + \bar{x}_i. \tag{5}$$

A coordinate transformation, $\{\bar{x}\} = [\nu]\{\eta\}$, and substitution into Eq. (4) with a premultiplication by $[\nu]^T$ yields:

$$\{\ddot{\eta}\} + [\diagdown \omega_i^2 \diagdown]\{\eta\} = -\frac{\ddot{u}_B(t)}{Nm}[\nu]^T\{M_i\}. \tag{6}$$

Duhamels integral solution gives:

$$\{\eta\} = -[\diagdown \omega_i \diagdown]^{-1}\int_0^t [\diagdown \sin \omega_i(t-\tau) \diagdown]\frac{\ddot{u}_B(\tau)}{Nm}[\nu]^T\{M_i\}d\tau. \tag{7}$$

Constant Base Acceleration:

Letting $\ddot{u}_B(t) = A_0 =$ constant, and using equation (7) gives:

$$\{\bar{x}\} = -\frac{A_0}{Nm}[\nu][\diagdown\omega_i\diagdown]^{-1}\left[\frac{\diagdown 1 - \cos\omega_i t\diagdown}{\omega_i}\right][\nu]^T\{M_i\} \quad (8)$$

Half Sine Pulse Base Acceleration:

Using a half sine pulse such that,

$$\left.\begin{aligned}\ddot{u}_B(t) &= A_0 \sin(t/t_1), \quad 0 \le t \le \pi t_1\\ &= 0 \qquad\qquad , \quad t \ge \pi t_1\end{aligned}\right\}. \quad (9)$$

Therefore, using equation (7) and substituting for $\ddot{u}_B(t)$ into it yields: For $0 \le t \le \pi t_1$,

$$\{\bar{x}\} = -\frac{A_0}{Nm}[\nu][\diagdown\omega_i\diagdown]^{-1} \times \left[\frac{\diagdown\omega_i \sin(t/t_1) - 1/t_1 \sin(\omega_i t)}{(\omega_i^2 - 1/t_1^2)\diagup}\right][\nu]^T\{M_i\}. \quad (10)$$

For $t \ge \pi t_1$,

$$\{\bar{x}\} = \frac{A_0}{Nm}[\nu][\diagdown\omega_i\diagdown]^{-1} \times \left[\frac{\diagdown\sin\omega_i(t - \pi t_1) + \sin(\omega_i t)}{t_1(\omega_i^2 - 1/t_1^2)\diagup}\right][\nu]^T\{M_i\}. \quad (11)$$

Consistent Mass Matrix Formulation

A Homogeneous Solutions. The basic difference between the lumped parameter description of the discrete problem and that of the consistent mass matrix is that the mass matrix for the latter case is nondiagonal. Hence, the homogeneous equations are the same as those for the lumped parameter models, or

$$[M]\{\ddot{x}\} + [K]\{x\} = \{0\} \quad (12)$$

where $[M]$ is a nondiagonal, positive definite matrix and can be broken into a product of upper and lower triangular matrices [13] of the form,

$$[M] = [B]^T[B]$$

where $[B]$ is an upper triangular matrix. Using a coordinate transformation $\{x\} = [B]^{-1}\{q\}$ and premultiplication by $[[B]^{-1}]^T$ reduces Eq. (12) to:

$$\{\ddot{q}\} + [\bar{K}]\{q\} = \{0\}, \quad (13)$$

where:

$$[\bar{K}] = [B^{-1}]^T[K][B]^{-1}.$$

Eigenvalues of equation (13) are the same as those of equation (12). The eigenvectors of equation (13) were transformed into the original coordinates of equation (12) and normalized by the same procedure as outlined in Section 2A.

B Forced Excitation Solutions. The equations of motion in matrix form are given by:

$$[M]\{\ddot{\bar{x}}\} + [K]\{\bar{x}\} = -\ddot{u}_B(t)[M][1, 1, \ldots, 1]^T. \quad (14)$$

It should be noted that this is of the same form as equation (4) except $[M]$ in equation (14) is nondiagonal and $[M]$ $[1, 1, \ldots, 1]^T$ replaces $\{M_i\}$. The orthogonality conditions do not depend upon the mass matrix being diagonal; hence, the solutions given in equations (8), (10), and (11) are applicable to the consistent mass matrix formulation if $\{M_i\}$ in these equations is replaced appropriately as shown in equation (14).

System Strain Energy

In matrix form the system strain energy for a discrete system is given by:

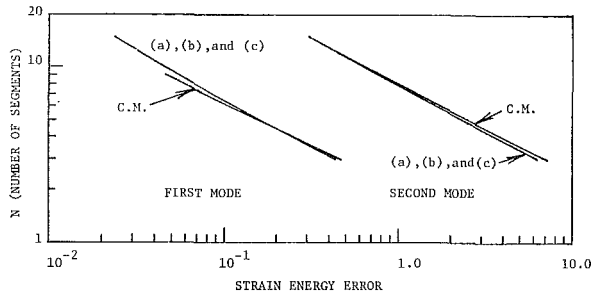

Fig. 3 One-dimensional maximum strain energy errors for fixed-fixed end conditions

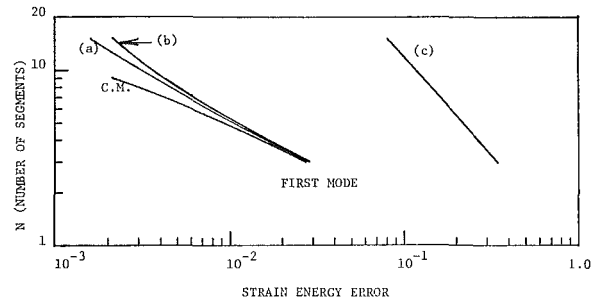

Fig. 4 One-dimensional maximum strain energy errors for fixed-free end conditions

$$U(t) = 1/2\{x\}^T[K]\{x\}. \quad (15)$$

In examining the strain energy for a given principal mode the displacement vector of equation (15) is replaced by the appropriate mode shape vector, $\{\nu\}_i$. Under forced excitation conditions $\{x\}$ in equation (15) is replaced by $\{\bar{x}(t)\}$, for a given model, from the appropriate solutions in equations (8), (10), or (11). Maximum system strain energy can be obtained by maximizing equation (15) over time.

In Appendix E the maximum system strain energy formulation for continuous systems is given. The maximum system strain energy obtained via the modeling techniques was subtracted from the continuous solution, in each appropriate case, to form strain energy errors.

Comparison of Results

A One-Dimensional Systems. Models (*a*) and (*b*) and the consistent mass matrix technique produce nearly the same strain energy errors in the lower order principal modes, see Figs. 3 and 4. When N is large the errors behave as $1/N^2$ for the boundary conditions investigated. Model (*c*) is less consistent under the same principal mode comparison; for fixed-fixed ends, the strain energy error behaves as $1/N^2$ while for fixed-free ends as $1/N$. The behavior of the strain energy error for all three models and the consistent mass matrix technique is similar to that based on the frequency root error comparison [3–5].

In extending the model comparison to transient behavior, model (*a*) and the consistent mass matrix technique were found to produce more consistent strain energy errors than models (*b*) and (*c*), see Fig. 5. For a constant base acceleration these errors behave approximately as $1/N^2$ while model (*c*) indicates errors nearly proportional to $1/N$ and model (*b*) slightly better than $1/N$ for values of N in the range 3, 5, and 9. This result is similar to that of the frequency root error behavior for the fixed-free case, except for model (*b*). Fig. 6 shows a case of the half-sine pulse type of base excitation. Fig. 6 indicates that model (*a*) and the consistent mass matrix approach produce errors slightly better than $1/N^2$ while models (*b*) and (*c*) are nearly proportional to $1/N$ for values of N in the range of 3 to 9. Results

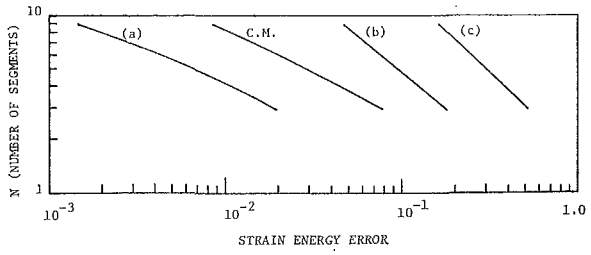

Fig. 5 One-dimensional maximum strain energy errors for constant base acceleration excitation

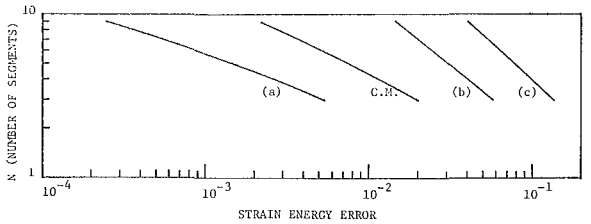

Fig. 6 One-dimensional maximum strain energy errors for half sine pulse base acceleration excitation (pulse duration = 25 percent of the fundamental period of the system)

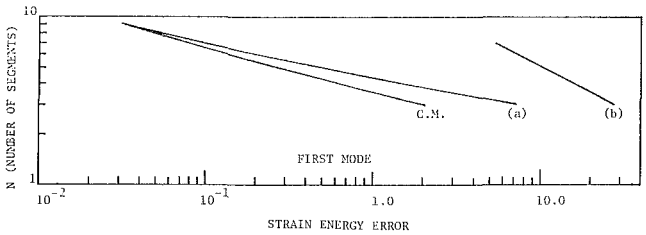

Fig. 7 Beam maximum strain energy errors for fixed-fixed end conditions (first mode)

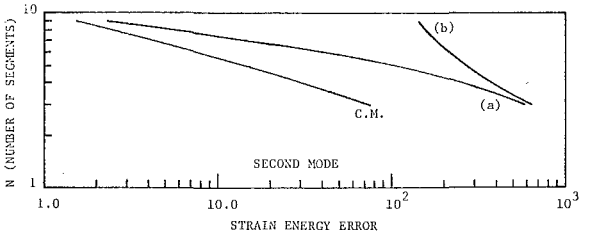

Fig. 8 Beam maximum strain energy errors for fixed-fixed end conditions (second mode)

similar to those indicated in Fig. 6 were obtained when a half sine pulse duration of 75 percent of the fundamental system period was used. While the convergence behavior of the maximum system strain energy has been the primary objective, it should be noted from Figs. 5 and 6 that the overall error level also varies from model to model. This latter point is of primary interest in most vibration analyses where N is usually small for each member of an overall structure.

B Bernoulli-Euler Beam. Figs. 7–9 show the strain energy errors for principal modes with fixed-fixed and fixed-free boundary conditions. The first three principal modes in each case were investigated. The general behavior of the error convergence is the same for all modes within a given set of boundary conditions with an overall shift in the error magnitude between modes. Figs. 7 and 8 illustrate this behavior for the first and second modes of a fixed-fixed beam.

The consistent mass matrix technique indicates error behavior which is nearly the same for both boundary conditions, wherein the lumped parameter errors are distinctly different. This is similar to previous comparisons of these modeling techniques based upon frequency root errors. Monotonic convergence was

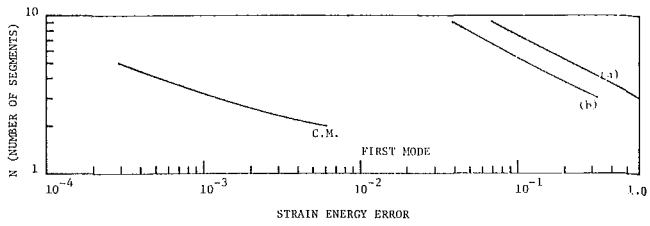

Fig. 9 Beam maximum strain energy errors for fixed-free end conditions

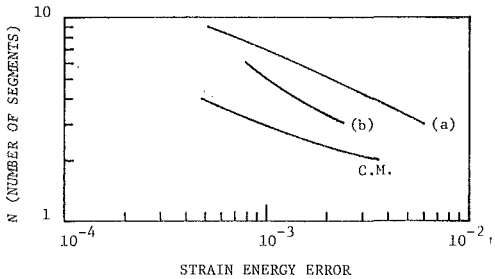

Fig. 10 Beam maximum strain energy errors for constant base acceleration excitation

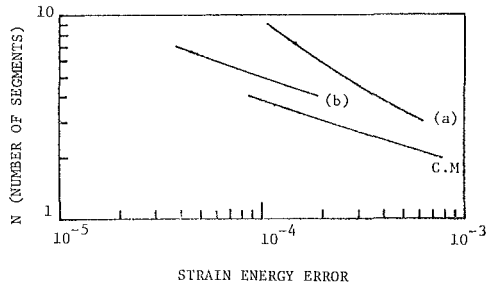

Fig. 11 Beam maximum strain energy errors for half-sine pulse base acceleration excitation (pulse duration = 25 percent of the fundamental period of the system)

not obtained for model (*b*) with fixed-fixed end conditions, as the convergence was oscillatory in nature. However, when the rotatory inertia terms were retained in the matrix equations, i.e., the reduction technique of Appendix D was not used, the errors decreased monotonically as N increased, see Fig. 7. This problem did not develop with model (*b*) for the fixed-free end conditions.

In comparing the models for a fixed-free beam with base acceleration, the consistent mass matrix technique was best in the cases examined. However, the results obtained using this technique do not greatly exceed those of the lumped parameter models (*a*) and (*b*) in these cases, as was evident in the principal mode comparison; see Figs. 10 and 11. The convergence of the strain energy errors under base excitation conditions is not as rapid as it was in the principal modes. The magnitude of the strain energy errors is smaller for models (*a*) and (*b*) under these dynamic conditions than in the principal modes.

Conclusions

Using the maximum system strain energy as the basis of comparison, lumped parameter models and the consistent mass matrix technique have been compared in describing one-dimensional and Bernoulli-Euler beam elements. In principal mode states, the results obtained are similar to those of previous comparisons, i.e., strain energy errors converge at the same rate as frequency root errors made for the modeling techniques considered.

In more general dynamic states, as illustrated by constant and half sine base acceleration excitation, the consistent mass matrix technique is not clearly the best. For one-dimensional systems model (*a*) gave errors of smaller magnitude, but which converged

at the same rate as the consistent mass technique. For Bernoulli-Euler beam elements the consistent mass matrix technique was slightly better than the best lumped parameter model. Based upon the limited number of cases treated herein, the authors feel that the better lumped parameter models and the consistent mass matrix technique are much more comparable for describing general forced excitation vibration than previous principal mode frequency root error analyses have indicated.

Acknowledgment

The research work of which this paper is a part was supported by the National Science Foundation under NSF Grant No. GK-4840.

References

1 Lagrange, J. L., *Analytique Mechanique*, 1788.

2 Rayleigh, J. W. S., *The Theory of Sound*, 2nd ed. rev., Vol. 1, Dover Publications, New York, 1945, pp. 172–177.

3 Duncan, J. W., "A Critical Examination of the Representation of Massive and Elastic Bodies by Rigid Masses Elastically Connected," *Quarterly Journal of Mechanics and Applied Mathematics*, Vol. 8, 1955, pp. 353–360.

4 Rocke, R. D., "Transmission Matrices and Lumped Parameter Models for Continuous Systems," Dynamics Laboratory Report, Calif. Institute of Technology, 1966, pp. 102–107.

5 Rocke, R. D., "Evaluation of Models for One-Dimensional Vibration Systems," 41st Shock and Vibration Bulletin, Oct. 1970.

6 Livesley, R. K., "The Equivalence of Continuous and Discrete Distributions in Certain Vibration Problems," *Quarterly Journal of Mechanics and Mathematics*, Vol. 8, 1955, pp. 353–360.

7 G. M. L., Gladwell, "The Approximation of Uniform Beams in Transverse Vibration by Sets of Masses Elastically Connected," Proc. 4th U. S. Nat'l. Congress of Applied Mechanics, 1962, pp. 169–176.

8 Leckie, F. A., and Lindberg, G. M., "The Effect of Lumped Parameters on Beam Frequencies," *Aeronautical Quarterly*, Vol. 14, 1963, pp. 224–240.

9 Lindberg, G. M., "Vibration of Non-Uniform Beams," *Aeronautical Quarterly*, Vol. 14, 1963, pp. 387–395.

10 Archer, J. S., "Consistent Mass Matrix for Distributed Mass Systems," *Journal of The Structural Division*, A.S.C.E., Vol. 89, No. ST4, Aug. 1963, pp. 161–178.

11 Krishna Murty, A. V., "A Lumped Inertia Force Method for Vibration Problems," *Aeronautical Quarterly*, May 1966, pp. 127–140.

12 Mains, R. M., "Comparison of Consistent Mass Matrix Schemes," *The Shock and Vibration Bulletin*, Bulletin 40, Part 4, Dec. 1969, pp. 1–16.

13 Benton, M. D., Hobbs, G. K., Dickerson, J. R., "Dynamic Analysis of Complex Structures," *The Shock and Vibration Bulletin*, Bulletin 37, Part 2, Jan. 1968, pp. 173–192.

APPENDIX A

Matrices for One-Dimensional Models

a) Fixed-Fixed End Conditions:

Models (a) and (c) ($(N-1)\times(N-1)$ matrices)

$$[M] = \begin{bmatrix} m & & 0 \\ & \ddots & \\ 0 & & m \end{bmatrix}, \quad [K] = \begin{bmatrix} 2k & -k & & 0 \\ -k & 2k & \ddots & \\ & \ddots & \ddots & -k \\ 0 & & -k & 2k \end{bmatrix}$$

Model (b) ($N \times N$ matrices)

$$[M] = \begin{bmatrix} m & & 0 \\ & \ddots & \\ 0 & & m \end{bmatrix}, \quad [K] = \begin{bmatrix} 3k & -k & & 0 \\ -k & 2k & \ddots & \\ & \ddots & \ddots & -k \\ 0 & & -k & 3k \end{bmatrix}$$

(*Continued in next column*)

b) Fixed-Free End Conditions:

Model (a) ($N \times N$ matrices)

$$[M] = \begin{bmatrix} m & & 0 \\ & \ddots & \\ 0 & & \frac{m}{2} \end{bmatrix}, \quad [K] = \begin{bmatrix} 2k & -k & & 0 \\ -k & 2k & \ddots & \\ & \ddots & \ddots & -k \\ 0 & & -k & k \end{bmatrix}$$

Model (b) ($N \times N$ matrices)

$$[M] = \begin{bmatrix} m & & 0 \\ & \ddots & \\ 0 & & m \end{bmatrix}, \quad [K] = \begin{bmatrix} 3k & -k & & 0 \\ -k & 2k & \ddots & \\ & \ddots & \ddots & -k \\ 0 & & -k & k \end{bmatrix}$$

Model (c) ($N \times N$ matrices)

$$[M] = \begin{bmatrix} m & & 0 \\ & \ddots & \\ 0 & & m \end{bmatrix}, \quad [K] = \begin{bmatrix} 2k & -k & & 0 \\ -k & 2k & \ddots & \\ & \ddots & \ddots & -k \\ 0 & & -k & k \end{bmatrix}$$

where: $k = \frac{AE}{\ell}$, $\ell = \frac{L}{N}$, and $m = \rho A \ell$.

APPENDIX B

Stiffness Matrices for Bernoulli-Euler Beam Models

a) Fixed-Fixed End Conditions:

Model (a)

$$[K] = \frac{2EI}{\ell^3} \cdot \left[\begin{array}{c|c} a & b \\ \hline c & d \end{array}\right] \quad (2N-2) \times (2N-2)$$

$$[a] = \begin{bmatrix} 12 & -6 & & 0 \\ -6 & 12 & \ddots & \\ & \ddots & \ddots & -6 \\ 0 & & -6 & 12 \end{bmatrix}, \quad [b] = \begin{bmatrix} 0 & -3\ell & & 0 \\ 3\ell & 0 & \ddots & \\ & \ddots & \ddots & -3\ell \\ 0 & & 3\ell & 0 \end{bmatrix}$$

$$[d] = \begin{bmatrix} 4\ell^2 & \ell^2 & & 0 \\ \ell^2 & 4\ell^2 & \ddots & \\ & \ddots & \ddots & \ell^2 \\ 0 & & \ell^2 & 4\ell^2 \end{bmatrix}, \quad [e] = \begin{bmatrix} 54 & -6 & & 0 \\ -6 & 12 & \ddots & \\ & \ddots & \ddots & -6 \\ 0 & & -6 & 54 \end{bmatrix}$$

$$[g] = \begin{bmatrix} 9\ell & 3\ell & & 0 \\ -3\ell & 0 & \ddots & \\ & \ddots & \ddots & 3\ell \\ 0 & & -3\ell & -9\ell \end{bmatrix}, \quad [h] = \begin{bmatrix} 6\ell^2 & \ell^2 & & 0 \\ \ell^2 & 4\ell^2 & \ddots & \\ & \ddots & \ddots & \ell^2 \\ 0 & & \ell^2 & 6\ell^2 \end{bmatrix}$$

Model (b)

$$[K] = \frac{2EI}{\ell^3} \cdot \left[\begin{array}{c|c} e & f \\ \hline g & h \end{array}\right] \quad (2N \times 2N)$$

$$[c] = \begin{bmatrix} 0 & 3\ell & & 0 \\ -3\ell & 0 & \ddots & \\ & \ddots & \ddots & 3\ell \\ 0 & & -3\ell & 0 \end{bmatrix}$$

$$[f] = \begin{bmatrix} 9\ell & -3\ell & & 0 \\ 3\ell & 0 & \ddots & \\ & \ddots & \ddots & -3\ell \\ 0 & & 3\ell & -9\ell \end{bmatrix}$$

b) Fixed-Free End Conditions:

Model (a)

$$[K] = \frac{2EI}{\ell^3} \cdot \left[\begin{array}{c|c} p & q \\ \hline r & s \end{array}\right] \quad (2N \times 2N)$$

$$[p] = \begin{bmatrix} 12 & -6 & & 0 \\ -6 & 12 & \ddots & \\ & \ddots & \ddots & -6 \\ 0 & & -6 & 6 \end{bmatrix}, \quad [q] = \begin{bmatrix} 0 & -3\ell & & 0 \\ 3\ell & 0 & \ddots & \\ & \ddots & \ddots & -3\ell \\ 0 & & 3\ell & 3\ell \end{bmatrix}$$

$$[s] = \begin{bmatrix} 4\ell^2 & \ell^2 & & 0 \\ \ell^2 & 4\ell^2 & \ddots & \\ & \ddots & \ddots & \ell^2 \\ 0 & & \ell^2 & 2\ell^2 \end{bmatrix}, \quad [u] = \begin{bmatrix} 54 & -6 & & 0 \\ -6 & 12 & \ddots & \\ & \ddots & \ddots & -6 \\ 0 & & -6 & 6 \end{bmatrix}$$

$$[w] = \begin{bmatrix} 9\ell & 3\ell & & 0 \\ -3\ell & 0 & \ddots & \\ & \ddots & \ddots & 3\ell \\ 0 & & -3\ell & 3\ell \end{bmatrix}, \quad [z] = \begin{bmatrix} 6\ell^2 & \ell^2 & & 0 \\ \ell^2 & 4\ell^2 & \ddots & \\ & \ddots & \ddots & \ell^2 \\ 0 & & \ell^2 & 2\ell^2 \end{bmatrix}$$

Model (b)

$$[K] = \frac{2EI}{\ell^3} \cdot \left[\begin{array}{c|c} u & v \\ \hline w & z \end{array}\right] \quad (2N \times 2N)$$

$$[r] = \begin{bmatrix} 0 & 3\ell & & 0 \\ -3\ell & 0 & \ddots & \\ & \ddots & \ddots & 3\ell \\ 0 & & -3\ell & 3\ell \end{bmatrix}$$

$$[v] = \begin{bmatrix} 9\ell & -3\ell & & 0 \\ 3\ell & 0 & \ddots & \\ & \ddots & \ddots & -3\ell \\ 0 & & 3\ell & 3\ell \end{bmatrix}$$

APPENDIX C

Consistent Mass Matrices for Fixed-Fixed and Fixed-Free Boundary Conditions

1. One-dimensional systems:

Fixed-Fixed End Conditions

$$[M] = \frac{\rho L}{6} \cdot \begin{bmatrix} 4 & 1 & & & 0 \\ 1 & 4 & \ddots & & \\ & \ddots & \ddots & 1 & \\ & & 1 & 4 & \\ 0 & & & 1 & 4 \end{bmatrix} \quad (N-1) \times (N-1)$$

Fixed-Free End Conditions

$$[M] = \frac{\rho L}{6} \cdot \begin{bmatrix} 4 & 1 & & & 0 \\ 1 & 4 & \ddots & & \\ & \ddots & \ddots & 1 & \\ & & 1 & 4 & \\ 0 & & & 1 & 2 \end{bmatrix} \quad (N \times N)$$

2. Bernoulli-Euler Beam

Fixed-Fixed End Conditions

$$[M] = \frac{\rho L}{420} \cdot \begin{bmatrix} [a'] & [b'] & & 0 \\ [c'] & [d'] & \ddots & \\ & \ddots & \ddots & [b'] \\ 0 & & [c'] & [d'] \end{bmatrix} \quad (2N-2) \times (2N-2)$$

Fixed-Free End Conditions

$$[M] = \frac{\rho L}{420} \cdot \begin{bmatrix} [a'] & [b'] & & 0 \\ [c'] & [d'] & \ddots & \\ & \ddots & \ddots & [e'] \\ 0 & & [f'] & [g'] \end{bmatrix} \quad (2N \times 2N)$$

$$[a'] = \begin{bmatrix} 312 & 54 & & & 0 \\ 54 & 312 & \ddots & & \\ & \ddots & \ddots & 54 & \\ & & 54 & 312 & \\ 0 & & & 54 & 312 \end{bmatrix}, \quad [b'] = \begin{bmatrix} 0 & 13L & & & 0 \\ -13L & 0 & \ddots & & \\ & \ddots & \ddots & 13L & \\ & & -13L & 0 & \\ 0 & & & -13L & 0 \end{bmatrix}, \quad [c'] = \begin{bmatrix} 0 & -13L & & & 0 \\ 13L & 0 & \ddots & & \\ & \ddots & \ddots & -13L & \\ & & 13L & 0 & \\ 0 & & & 13L & 0 \end{bmatrix}$$

$$[d'] = \begin{bmatrix} 8L^2 & -3L^2 & & & 0 \\ -3L^2 & 8L^2 & \ddots & & \\ & \ddots & \ddots & -3L^2 & \\ & & -3L^2 & 8L^2 & \\ 0 & & & -3L^2 & 8L^2 \end{bmatrix}, \quad [e'] = \begin{bmatrix} 312 & 54 & & & 0 \\ 54 & 312 & \ddots & & \\ & \ddots & \ddots & 54 & \\ & & 54 & 312 & \\ 0 & & & 54 & 156 \end{bmatrix}, \quad [f'] = \begin{bmatrix} 0 & 13L & & & 0 \\ -13L & 0 & \ddots & & \\ & \ddots & \ddots & 13L & \\ & & -13L & 0 & \\ 0 & & & -13L & 22L \end{bmatrix}$$

$$[g'] = \begin{bmatrix} 0 & -13L & & & 0 \\ 13L & 0 & \ddots & & \\ & \ddots & \ddots & -13L & \\ & & 13L & 0 & \\ 0 & & & 13L & 22L \end{bmatrix}, \quad [h'] = \begin{bmatrix} 8L^2 & -3L^2 & & & 0 \\ -3L^2 & 8L^2 & \ddots & & \\ & \ddots & \ddots & -3L^2 & \\ & & -3L^2 & 8L^2 & \\ 0 & & & -3L^2 & 4L^2 \end{bmatrix}$$

APPENDIX D

Reduction of Equations to Eliminate Rotary Inertia Terms

The governing homogeneous differential equations for the Bernoulli-Euler lumped parameter models can be partitioned to the form:

$$\begin{bmatrix} [M] & 0 \\ 0 & [J] \end{bmatrix} \begin{Bmatrix} \ddot{y} \\ \ddot{\theta} \end{Bmatrix} + \begin{bmatrix} [K_{11}] & [K_{12}] \\ [K_{21}] & [K_{22}] \end{bmatrix} \begin{Bmatrix} y \\ \theta \end{Bmatrix} = \begin{Bmatrix} 0 \\ 0 \end{Bmatrix}. \quad (16)$$

For the lower modes of a uniform beam it can be shown that $J_i\ddot{\theta}_i \ll M_i\ddot{y}_i$; hence for reduction of equation $J_i\ddot{\theta}_i \approx 0$ and

$$[M]\{\ddot{y}\} + [K_{11}]\{y\} + [K_{12}]\{\theta\} = \{0\}, \text{ and} \quad (17)$$

$$[K_{21}]\{y\} + [K_{22}]\{\theta\} = \{0\}. \quad (18)$$

Equation (18) gives:

$$\{\theta\} = -[K_{22}]^{-1}[K_{21}]\{y\}.$$

Substituting this into equation (17) gives:

$$[M]\{\ddot{y}\} + [\tilde{K}]\{y\} = \{0\} \quad (19)$$

where:

$$[\tilde{K}] = -[K_{12}][K_{22}]^{-1}[K_{21}] + [K_{11}]$$

APPENDIX E

Strain Energy Formulation for Continuous Systems

1 One-Dimensional Systems

$$\text{System strain energy} = U(t) = \tfrac{1}{2}\int_0^L EA\left[\frac{\partial u(x,t)}{\partial x}\right]^2 dx. \quad (20)$$

(a) Principal Modes

Fixed-Fixed End Conditions. The displacement function $u(x, t)$ can be written as $u(x, t) = \Phi_n(x)f_n(t)$, where $f_n(t)$ is sinusoidal and the mode shapes $\Phi_n(x)$ for fixed-fixed end conditions are given by:

$$\Phi_n(x) = D_n \sin(n\pi x/L).$$

The normalization constant D_n was obtained by normalizing the first orthogonality relation to the total mass of the bar,

$$\int_0^L \rho\Phi_n^2(x)dx = \rho L.$$

$$\therefore D_n = \left[L \Big/ \int_0^L \sin^2(n\pi x/L)dx\right]^{1/2} = \sqrt{2}.$$

Hence, strain energy in the nth mode is given by:

$$U_n = \tfrac{1}{2}EA\int_0^L 2\cdot\left(\frac{n\pi}{L}\right)^2 \cos^2(n\pi x/L)dx = \frac{EA}{2L}(n\pi)^2 \quad (21)$$

Fixed-Free End Conditions.

$$\Phi_n(x) = D_n \sin[(2n-1)\pi x/2L], \; D_n = \sqrt{2}.$$

$$\therefore U_n = \frac{EA}{8L}[(2n-1)\pi]^2. \quad (22)$$

(b) Strain Energy in Forced Excitation.

For constant base acceleration, the displacement solution is:

$$u(x, t) = \frac{-16A_0\rho L^2}{\pi^3 AE} \sum_{n=1,3,5..} \frac{1}{n^3} \cdot\left[1 - \cos\left(\frac{n\pi t}{2}\sqrt{AE/\rho L^2}\right)\right]\sin\left(\frac{n\pi x}{2L}\right). \quad (23)$$

Substitution into equation (20) yields:

$$U(t) = \frac{32AE}{\pi^4}\left(\frac{A_0\rho L}{AE}\right)^2 \int_0^L A(x, t)\cdot B(x, t)dx$$

where:

$$A(x, t) = \sum_{n=1,3,5..} \frac{1}{n^2} \cdot\left\{1 - \cos\left(\frac{n\pi t}{2}\sqrt{AE/\rho L^2}\right)\right\}\cos(n\pi x/2L)$$

$$B(x, t) = \sum_{p=1,3,5..} \frac{1}{p^2} \cdot\left\{1 - \cos\left(\frac{p\pi t}{2}\sqrt{AE/\rho L^2}\right)\right\}\cos(p\pi x/2L).$$

Using orthogonality and normalization relations,

$$\int_0^L \frac{\partial\Phi_n(x)}{\partial x}\cdot\frac{\partial\Phi_p(x)}{\partial x}\cdot dx = \begin{cases} 0, & n \neq p \\ \displaystyle\int_0^L \left[\frac{\partial\Phi_n(x)}{\partial x}\right]^2\cdot dx, & n = p \end{cases} \quad (24)$$

the system strain energy becomes:

$$U(t) = \frac{16AEL}{\pi^4}\left(\frac{A_0\rho L}{AE}\right)^2 \sum_{n=1,3,5..} \frac{1}{n^4} \cdot\left[1 - \cos\left(\frac{n\pi t}{2}\sqrt{AE/\rho L^2}\right)\right]^2 \quad (25)$$

and at $t = 2\sqrt{\rho L^2/AE}$,

$$U_{\max} = \frac{64A_0^2\rho^2L^3}{\pi^4AE} \sum_{n=1,3,5..} \left(\frac{1}{n^4}\right) = \frac{2A_0^2\rho^2L^3}{3AE}. \quad (26)$$

For the half sine pulse base acceleration excitation during $0 \leq t \leq \pi t_1$:

$$u(x, t) = \frac{-8A_0}{\pi^2}\sqrt{\frac{\rho L^2}{AE}} \sum_{n=1,3,5..} \frac{1}{n^2} \times \frac{\left[\frac{n\pi}{2L}\sqrt{\frac{AE}{\rho}} \sin(t/t_1) - \frac{1}{t_1} \sin\left(\frac{n\pi t}{2L}\sqrt{\frac{AE}{\rho}}\right)\right]}{\left[\left(\frac{n\pi}{2L}\sqrt{\frac{AE}{\rho}}\right)^2 - \frac{1}{t_1^2}\right]} \sin\left(\frac{n\pi x}{2L}\right), \quad (27)$$

and the strain energy is:

$$U(t) = \frac{4A_0^2\rho L}{\pi^2} \sum_{n=1,3,5..} \frac{1}{n^2} \times \frac{\left[\frac{n\pi}{2L}\sqrt{\frac{AE}{\rho}} \sin(t/t_1) - \frac{1}{t_1} \sin\left(\frac{n\pi t}{2L}\sqrt{\frac{AE}{\rho}}\right)\right]^2}{\left[\left(\frac{n\pi}{2L}\sqrt{\frac{AE}{\rho}}\right)^2 - \frac{1}{t_1^2}\right]^2}. \quad (28)$$

For $t \geq \pi t_1$:

$$u(x, t) = \frac{8A_0}{\pi^2 t_1}\sqrt{\frac{\rho L^2}{AE}} \sum_{n=1,3,5..} \frac{1}{n^2} \times \frac{\left[\sin\frac{n\pi}{2L}\sqrt{\frac{AE}{\rho}}(t - \pi t_1) + \sin\left(\frac{n\pi t}{2L}\sqrt{\frac{AE}{\rho}}\right)\right]}{\left[\left(\frac{n\pi}{2L}\sqrt{\frac{AE}{\rho}}\right)^2 - \frac{1}{t_1^2}\right]} \sin\left(\frac{n\pi x}{2L}\right) \quad (29)$$

and the strain energy is:

$$U(t) = \frac{4A_0^2\rho L}{\pi^2 t_1^2} \sum_{n=1,3,5..} \frac{1}{n^2} \times \frac{\left[\sin\frac{n\pi}{2L}\sqrt{\frac{AE}{\rho}}(t - \pi t_1) + \sin\left(\frac{n\pi t}{2L}\sqrt{\frac{AE}{\rho}}\right)\right]^2}{\left[\left(\frac{n\pi}{2L}\sqrt{\frac{AE}{\rho}}\right)^2 - \frac{1}{t_1^2}\right]^2}. \quad (30)$$

2 Bernoulli-Euler Beam.

$$\text{System strain energy} = U(t) = {}^1/_2 \int_0^L EI\left[\frac{\partial^2 y(x, t)}{\partial x^2}\right]^2 dx. \quad (31)$$

(a) Principal Modes

Fixed-Fixed End Conditions. For fixed-fixed end conditions the displacement of the beam in the rth mode is given by: $y_r(x, t) = \Phi_r(x)f_r(t)$ where $f_r(t)$ is sinusoidal and the mode shapes $\Phi_r(x)$ are given by:

$$\Phi_r(x) = \cosh(\lambda_r x) - \cos(\lambda_r x) - \sigma_r[\sinh(\lambda_r x) - \sin(\lambda_r x)] \quad (32)$$

where:

$$\sigma_r = \frac{\cosh(\lambda_r L) - \cos(\lambda_r L)}{\sinh(\lambda_r L) - \sin(\lambda_r L)}.$$

The λ_r are obtained from the transcendental equation

$$\cosh(\lambda_r L)\cos(\lambda_r L) = 1.$$

Using equations (31) and (32), the maximum system strain energy becomes:

$$U_{r_{\max}} = \frac{EI}{2}\int_0^L \left[\frac{d^2\Phi_r(x)}{dx^2}\right]^2 dx$$

where:

$$\left(\frac{d^2\Phi_r(x)}{dx^2}\right)^2 = \lambda_r^4[(\cosh\lambda_r x + \cos\lambda_r x)^2 + \sigma_r^2(\sinh\lambda_r x + \sin\lambda_r x)^2 - 2\sigma_r(\cosh\lambda_r x + \cos\lambda_r x) \times (\sinh\lambda_r x + \sin\lambda_r x)].$$

Therefore:

$$U_{r_{\max}} = \frac{EI}{2}\lambda_r^3\psi_r(\lambda_r, \sigma_r)$$

where:

$$\psi_r(\lambda_r, \sigma_r) = [\lambda_r L + (1 + \sigma_r)^2\{{}^1/_4\sinh 2\lambda_r L + \cosh\lambda_r L\sin\lambda_r L\} + (1 - \sigma_r)^2\{{}^1/_4\sin 2\lambda_r L + \sinh\lambda_r L\cos\lambda_r L\} - 2\sigma_r\{{}^1/_4(\cosh 2\lambda_r L - \cos\lambda_r L) + \sinh\lambda_r L\sin\lambda_r L\}]. \quad (33)$$

Fixed-Free End Conditions. Maximum system strain energy is given by the same expression as that for the fixed-fixed end conditions except that for this case:

$$\sigma_r = \frac{\sinh\lambda_r L - \sin\lambda_r L}{\cosh\lambda_r L - \cos\lambda_r L}$$

and the λ_r are obtained from:

$$\cosh(\lambda_r L)\cos(\lambda_r L) = -1.$$

(b) Strain Energy in Forced Excitation. The system strain energy is given by:

$$U(t) = \frac{EI}{2}\int_0^L \left[\frac{\partial^2 y(x, t)}{\partial x^2}\right]^2 \cdot dx$$

where $y(x, t)$ can be written as $y(x, t) = \sum_{n=1}^{\infty} \Phi_n(x)f_n(t)$.

Therefore:

$$U(t) = \frac{EI}{2}\int_0^L \left\{\sum_{n=1}^{\infty}\frac{d^2\Phi_n(x)}{dx^2}f_n(t)\right\} \times \left\{\sum_{p=1}^{\infty}\frac{d^2\Phi_p(x)}{dx^2}f_p(t)\right\} dx = \frac{EI}{2}\sum_{n=1}^{\infty}\sum_{p=1}^{\infty} f_n(t)f_p(t)\int_0^L \frac{d^2\Phi_n(x)}{dx^2}\cdot\frac{d^2\Phi_p(x)}{dx^2}dx. \quad (34)$$

Using orthogonality relations:

$$\left.\begin{aligned}\int_0^L \frac{d^2\Phi_n(x)}{dx^2}\cdot\frac{d^2\Phi_p(x)}{dx^2}\cdot dx &= 0, & n \neq p\\ &= \int_0^L \left(\frac{d^2\Phi_n(x)}{dx^2}\right)^2 dx, & n = p\end{aligned}\right\} \quad (35)$$

the system strain energy becomes:

$$U(t) = \frac{EI}{2}\sum_{n=1}^{\infty} f_n^2(t)\int_0^L \left(\frac{d^2\Phi_n(x)}{dx^2}\right)^2 dx. \quad (36)$$

Constant Base Acceleration. The time dependent part of the solution for a constant base acceleration excitation is given by:

$$f_n(t) = \frac{2\sigma_n A_0}{\lambda_n L\omega_n^2}[1 - \cos(\omega_n t)]. \quad (37)$$

Therefore:

$$U(t) = \frac{2EIA_0^2}{L^2} \sum_{n=1}^{\infty} \frac{\sigma_n^2 \lambda_n}{\omega_n^4} [1 - \cos(\omega_n t)]^2 \psi_n(\lambda_n, \sigma_n) \quad (38)$$

where $\psi_n(\lambda_n, \sigma_n)$ is given by equation (33).

Half Sine Pulse Base Acceleration. For a half sine pulse base acceleration during $0 \leq t \leq \pi t_1$:

$$f_n(t) = \frac{-2\sigma_n A_0}{\lambda_n \omega_n L} \frac{\left[\omega_n \sin(t/t_1) - \frac{1}{t_1} \sin(\omega_n t)\right]}{\left[\omega_n^2 - \frac{1}{t_1^2}\right]}. \quad (39)$$

Therefore:

$$U(t) = \frac{2EIA_0^2}{L^2} \sum_{n=1}^{\infty} \frac{\sigma_n^2 \lambda_n}{\omega_n^2} \frac{\left[\omega_n \sin(t/t_1) - \frac{1}{t_1} \sin(\omega_n t)\right]^2}{\left[\omega_n^2 - \frac{1}{t_1^2}\right]^2} \cdot \psi_n(\lambda_n, \sigma_n). \quad (40)$$

For $t \geq \pi t_1$:

$$f_n(t) = \frac{-2\sigma_n A_0}{\lambda_n \omega_n L} \frac{[\sin \omega_n(t - \pi t_1) + \sin(\omega_n t)]}{t_1 \left[\omega_n^2 - \frac{1}{t_1^2}\right]} \quad (41)$$

Therefore:

$$U(t) = \frac{2EIA_0^2}{L^2 t_1^2} \sum_{n=1}^{\infty} \frac{\sigma_n^2 \lambda_n}{\omega_n^2} \frac{[\sin \omega_n(t - \pi t_1) + \sin(\omega_n t)]^2}{\left[\omega_n^2 - \frac{1}{t_1^2}\right]^2} \cdot \psi_n(\lambda_n, \sigma_n) \quad (42)$$

where λ_n and σ_n are obtained from fixed-free case of section 2(*a*) in the foregoing.